HHS Public Access

Author manuscript

Sci Transl Med. Author manuscript; available in PMC 2015 November 27.

Published in final edited form as:

Sci Transl Med. 2015 May 27; 7(289): 289ra86. doi:10.1126/scitranslmed.aaa8103.

SLC7A11 expression is associated with seizures and predicts poor survival in patients with malignant glioma

Stephanie M. Robert[1], **Susan C. Buckingham**[1], **Susan L. Campbell**[1], **Stefanie Robel**[1], **Kenneth T. Holt**[1], **Toyin Ogunrinu-Babarinde**[1], **Paula Province Warren**[2], **David M. White**[3], **Meredith A. Reid**[3], **Jenny M. Eschbacher**[4], **Michael E. Berens**[4], **Adrienne C. Lahti**[3], **Louis B. Nabors**[2], and **Harald Sontheimer**[1,*]

[1]Department of Neurobiology, Center for Glial Biology in Medicine, University of Alabama at Birmingham, Birmingham, AL, 35294, USA

[2]Division of Neuro-oncology, University of Alabama at Birmingham, Birmingham, AL, 35294, USA

[3]Department of Psychiatry and Behavioral Neurobiology, The University of Alabama at Birmingham, Birmingham, AL, 35294, USA

[4]Cancer and Cell Biology Division, The Translational Genomics Research Institute (TGen), Phoenix, AZ, 85004, USA

Abstract

Glioma is the most common malignant primary brain tumor. Their rapid growth is aided by tumor-mediated release of glutamate, creating peritumoral excitotoxic cell death and vacating space for tumor expansion. Glioma glutamate release may also be responsible for seizures, which complicate the clinical course for many patients and are often the presenting symptom. A hypothesized glutamate release pathway is the cystine/glutamate transporter System x_c^- (SXC), responsible for the cellular synthesis of glutathione. However, the relationship of SXC-mediated glutamate release, seizures, and tumor growth remains unclear. Probing expression of SLC7A11/xCT, the catalytic subunit of SXC, in patient tissue and tissues propagated in mice, we found that approximately 50% of patient tumors have elevated SLC7A11 expression. Compared with tumors lacking this transporter, *in vivo* propagated and intracranially implanted SLC7A11-expressing tumors grew faster, produced pronounced peritumoral glutamate excitotoxicity, induced seizures, and shortened overall survival. In agreement with animal data, increased SLC7A11 expression predicted shorter patient survival according to annotated genomic data in the REMBRANDT database. In a clinical pilot study we used Magnetic Resonance Spectroscopy (MRS) to determine SXC-mediated glutamate release by measuring acute changes in glutamate after administration of

*1719 6th Ave S.CIRC 425, Birmingham, AL, 35294; Phone: (205)-975-5805; Fax: (205)-975-6320; sontheimer@uab.edu.

Author contributions: S.M.R. designed, performed, analyzed the experiments, and wrote the manuscript; S.C.B. performed EEG experiments and data analysis; S.L.C. performed electrophysiology experiments; S.R. performed and analyzed EM images; K.T.H. contributed to Western blots and glutamate assay experiments; T.O.B. was involved in data analysis and planning of experiments; P.P.W. collected and analyzed patient data; D.M.W. and M.A.R. collected and analyzed MRS data; J.E. and M.E.B. collected, performed, and analyzed TMA data; A.C.L. oversaw MRS data acquisition and analysis; L.B.N. oversaw pilot clinical trial patient data acquisition and analysis; H.S. coordinated and directed the project, discussed the results and wrote the manuscript.

Competing interests: H. S. holds a patent on methods for treating glioma, US 8748445 B2. All other authors declare that they have no competing interests.

the FDA-approved SXC inhibitor, sulfasalazine. In 9 glioma patients with biopsy-confirmed expression of SXC, we found that its expression positively correlates with glutamate release, which is acutely inhibited with oral sulfasalazine. These data suggest that SXC is the major pathway for glutamate release from gliomas and that SLC7A11 expression predicts accelerated growth and peritumoral seizures.

Introduction

Malignant glioma is the most common and lethal primary brain tumor, and in dire need for more effective therapy. Gliomas display aggressive growth and diffuse invasion, with headaches and seizures being common presenting symptoms. Recently, the excitatory amino acid glutamate has been implicated in glioma etiology; a microdialysis study in glioma patients reported extracellular glutamate concentrations to be elevated >100-fold(1). The glioma-released glutamate has been suggested to enhance tumor invasion and aid growth by killing surrounding neurons through glutamate excitotoxicity(2), a pathway of cell death more commonly associated with stroke and neurodegenerative disease(3, 4). Glutamate release from gliomas has also been suggested to cause tumor-associated seizures (TAS)(5, 6), which affect up to half of all glioma patients(7, 8). TAS require treatment with one or more anti-epileptic drugs (AED), which produce undesirable side effects and potential drug interactions with chemotherapy treatments(9), and are often ineffective to control seizures in many patients.

One emerging hypothesis posits that glioma glutamate release is a consequence of enhanced self-preservation by tumor cells. Through an upregulation of a cystine/glutamate exchanger, System x_c^- (SXC)(10), many malignant cells, including those of gliomas, increase cystine uptake for intracellular synthesis of glutathione (GSH), an antioxidant that supports tumor growth and survival(11–13). SXC expression is regulated by the cellular redox state and is induced in gliomas under hypoxic conditions(11). Cystine uptake is energetically driven by glutamate release(14), which therefore becomes an obligatory byproduct of GSH synthesis. Elevated extracellular glutamate concentrations are well known to cause excitotoxic neuronal injury in stroke(15, 16) and seizures in epilepsy(17, 18).

SXC is the preferred of many possible pathways for glioma glutamate release and one that could be targeted pharmacologically, should SXC be confirmed to play a major role in the disease. One FDA-approved SXC inhibitor already exists (sulfasalazine(19)), and others are being developed(20).

By examining SXC expression in patient-derived gliomas, we have identified two subgroups that either highly express or essentially lack expression of SLC7A11 (also known as xCT), the catalytic subunit responsible for SXC-mediated glutamate release. When these glioma tissues were propagated *in vivo* as flank tumor xenolines(21, 22) and subsequently implanted intracranially, tumors with increased SLC7A11 expression caused tumor-associated seizures, peritumoral excitotoxicity, and shortened survival. Increased SLC7A11 was similarly associated with shortened patient survival in REMBRANDT, an annotated genomic glioma database. In a clinical pilot trial with 9 glioma patients, we used Magnetic Resonance Spectroscopy to identify patients whose tumors highly express SLC7A11, by

detecting changes in peritumoral glutamate release after sulfasalazine administration. Tissue expression of SLC7A11 positively correlated with sulfasalazine-sensitive glutamate release.

Results

SLC7A11 expression identifies two major glioma subtypes

The focus of this study was to determine if SXC-mediated glutamate release from malignant gliomas is responsible for peritumoral excitotoxic tissue destruction and tumor-associated seizures. The catalytic subunit of SXC, SLC7A11, is required for cystine and glutamate transport via the heteromeric SXC transporter. Because approximately 50–60% of glioma patients report seizures, we hypothesized that the expression of *SLC7A11*, the gene encoding the catalytic subunit of the SXC transporter, may vary in expression between patients, causing heterogeneous clinical sequelae.

To examine the expression of SXC across glioma patients, we studied SLC7A11 protein expression in glioblastoma multiforme (GBM), high-grade glioma, using tissue micro-arrays (TMAs) of matched tumor and peritumoral brain tissue from 41 patients. Unlike ordinary biopsies, which rarely provide access to non-tumor brain, these TMAs allow comparison of tumor versus peritumoral brain, matched for each patient. TMAs were incubated with antibodies against SLC7A11, scored in blinded fashion by a pathologist, and analyzed relative to those of each individual's matched, peritumoral brain. Analysis of tumor cores indicates a continuum of SLC7A11 expression (Fig. 1, A, B); however, both Gaussian fits to the expression data, and testing for departure from unimodality in the population (Hartigans' dip test; Peritumoral expression P=0.4757, GBM core expression P=0.01626) support the segregation of the patient tumors into high and low SXC expressers, relative to the average expression of SLC7A11 in the peritumoral tissue, which represents normal brain levels. Overall, there is significantly elevated expression in 53.7% of patient tumors relative to average peritumoral brain (High, 1.169±0.164, P<0.0001, *n*=21 patients), and low, almost undetectable SLC7A11 in the 46.3% with equal or lower expression compared to average peritumoral brain (Low, 0.083±0.016, *n*=20 patients; Peritumoral brain, 0.259±0.057, *n*=34). Similarly, 59.5% of the samples showed increased SLC7A11 expression in the tumor rim/edge (1.17±0.15; *n*=22 patients) (fig. S1). Elevated levels of this transporter near the tumor border may enhance the ability of glutamate released from SXC to reach and affect peritumoral brain.

Western blots from patient GBM tissue identified a similar expression profile for SLC7A11, with a little more than 50% of the tumors highly expressing SLC7A11 (6/11), the remaining ones showing almost undetectable SLC7A11 expression (5/11)(Fig. 1C). For further study, we selected 2 GBM patient tumors with high SLC7A11 expression (GBM22 and GBM1066; red) and 2 with low or no SLC7A11 expression (GBM14 and GBM39; blue), and maintained them as flank-propagated xenolines *in vivo* (fig. S2A, inset) for further functional evaluation. This method of tumor propagation preserves gene and protein expression of the original excised patient tumors(21–23). We confirmed that SLC7A11 expression was invariant during subsequent passaging in mice (fig. S2, A, B), as well as in cells maintained as gliospheres (GS) in short-term culture, and after subsequent intracranial (IC) implantation (fig. S2C). Furthermore, SLC7A11 immunocytochemistry confirms

membrane-associated expression, co-localizing with phalloidin, in GBM22 & GBM1066 gliomas and a lack of membrane expression in GBM14 & GBM39 gliomas (fig. S2D).

SLC7A11 expression by Western blot predicted functional SXC expression as determined through transport assays. Here, the SXC inhibitor (S)-4-carboxyphenylglycine ((S)-4-CPG) selectively blocked glutamate release in SLC7A11-expressing GBM22 & GBM1066 gliomas (Fig. 1D), but not in GBM14 & GBM39 gliomas, which express little SLC7A11. The auto-fluorescence of the SXC inhibitor sulfasalazine (SAS) interferes with the glutamate assay; therefore we examined transporter activity measuring reverse transport of ^{3}H-glutamate, confirming that SAS- and (S)-4-CPG-sensitive glutamate transport occurs only in SXC-expressing gliomas (Fig. 1E).

SXC activity produces excessive neuronal excitotoxicity

We next used ratiometric Fura-2 Ca^{2+} imaging to determine if glutamate released from SXC-expressing gliomas activates neuronal glutamate receptors, causing excitotoxicity. Cortical neurons showed intracellular Ca^{2+} increases averaging 299.4 ± 43.9 nM (n=4 independent experiments per condition; two-tailed, unpaired t-test, $P<0.01$) when exposed to SXC-expressing gliosphere-conditioned medium, which were greatly reduced by the glutamate receptor antagonist MK-801 and reduced even further by MK-801 combined with the AMPA/kainate receptor antagonist CNQX. A similar attenuation in Ca^{2+} was observed after SXC inhibition with (S)-4-CPG (Fig. 1F, fig. S3). In contrast, neurons exposed to conditioned medium harvested from non-SXC-expressing gliomas showed significantly ($P=0.0056$) smaller glutamate-mediated Ca^{2+} increases, averaging only 109.1±37.5 nM (Fig. 1F, fig. S3). These results suggest that glutamate release from SXC-expressing gliomas induces peritumoral neuronal Ca^{2+} responses.

To assess whether glutamate release is of sufficient magnitude to cause excitotoxicity, we co-cultured gliomas and cortical neurons using a transwell system, creating a barrier in which cells share medium without physical contact (fig. S4A). Neurons co-cultured with SXC-expressing gliospheres for 48 h showed a significant decrease (GBM22, $P=0.0035$; GBM1066, $P=0.0478$) in neuronal viability that was prevented by inhibition of SXC with either SAS or (S)-4-CPG, or blockade of neuronal glutamate receptors with MK-801 (fig. S4B).

We next assessed whether SXC-expressing tumors also induce excitotoxicity *in vivo* by implanting either SXC-expressing or non-SXC-expressing glioma cells intracranially into immune-deficient (*scid*) mice (1.5×10^{5} GBM cells/mouse). We observed an ~80% reduction in the number of peritumoral NeuN+ neurons in SXC-expressing glioma-implanted mice (Fig. 2, A, B, fig. S5) compared to the contralateral brain (fig. S6) or mice implanted with non-SXC-expressing gliomas. By contrast, GFAP+ astrocytes were equally surrounding tumors of both types (Fig. 2A, fig. S5), indicating that glutamate release does not affect peritumoral astrocytes. The observed reduction of NeuN+ neurons, presumably by excitotoxicity, was not replicated by intracranial injection of non-malignant astrocytes derived from Aldh1l1-EGFP- mice into *scid* mice (fig. S7).

The mean survival of mice bearing SXC-expressing gliomas was shortened to 20–22 days post-injection (dpi), compared to 27–32 dpi for those with non-SXC-expressing tumors (Fig. 2C). SXC-expressing glioma cells also grew faster *in vitro* (fig. S8A).

Histologically, SXC-expressing tumors have less distinct margins and show greater peritumoral invasion than non-SXC-expressing tumors, with significantly more cells migrating away from the tumor mass (GBM14, 679.9±18.84 cells/mm^2; n=3 animals; GBM22, 723.3±141.3 cells/mm^2, n=3 animals, f-test to compare variances, P=0.0350) (Fig. 2D, fig. S8B, fig. S9A). Electron microscopic (EM) images of tumor and peritumoral brain also illustrate interstitial edema, elaborate cellular processes, and flat, elongated cells in SXC-expressing gliomas. There was comparatively less edema in tissue samples containing non-SXC-expressing gliomas, where tumor cells appeared more round, with smaller protrusions and more distinguishable tumor borders (Fig. 2E, fig. S9B).

SXC-expressing gliomas enhance peritumoral neuronal hyperexcitability

Previous studies suggested that SXC-mediated glutamate release might be a factor in tumor-associated epilepsy(5). We therefore assessed the electrophysiological properties of peritumoral neurons in SXC-expressing and non-SXC-expressing glioma-implanted mice compared to sham controls. As shown by whole-cell patch-clamp recordings of layer II/III pyramidal neurons, neurons peritumoral to SXC-expressing gliomas showed more depolarized resting membrane potentials than shams, whereas those implanted with non-SXC-expressing gliomas did not (Fig. 3A). The input resistance and amplitude of the sag due to the inward rectifier cationic current (I_H) was not significantly different among the groups (Table 1). In current clamp, held at −70 mV, neurons peritumoral to SXC-expressing gliomas, but not peritumoral to non-SXC-expressing gliomas, fired significantly more action potentials (80 pA, P=0.0365; 100 pA, P=0.0384) at increasing current injections, compared to neurons in sham control slices (Fig. 3, B, C). Single action potentials (AP) showed no differences in amplitude, half width, and after-hyperpolarization (AHP)(Table 1). In current clamp, neurons were stepped to depolarizing potentials, comparing the threshold at which the first action potential occurred. No difference was found between the three groups (fig. S10), suggesting no change in the intrinsic excitability of neurons peritumoral to SXC-expressing gliomas. Hence an extrinsic factor, presumably glutamate, must be responsible for the enhanced excitability of these neurons. Table 1 summarizes all membrane parameters analyzed for the three groups.

To assess whether SXC expression influences the hyperexcitability threshold, we induced epileptiform activity using two well-established and widely-used pharmacological models, namely bicuculline and magnesium-free induced excitability(24, 25)(Fig. 3). We recorded spontaneous postsynaptic currents in artificial cerebrospinal fluid (ACSF) before and after bath application of the $GABA_A$ receptor blocker bicuculline (Bic, 10 μM). Epileptiform activity was rapidly induced in SXC-expressing tumor-bearing slices, whereas a much longer latency was required for activity in neurons in non-SXC-expressing tumor-bearing slices and sham controls (Fig. 3, D, F). Similarly, there was a shorter latency to the first epileptiform event in magnesium-free ACSF in the SXC-expressing tumor-bearing slices compared to non-SXC-expressing and sham control slices (Fig. 3, E, G). In addition, a larger

percentage of neurons in SXC-expressing tumor-bearing slices displayed epileptiform events after 30 min, compared to neurons in non-SXC-expressing and sham slices (Fig. 3H).

Because epilepsy requires network activation, we evaluated whether SXC-mediated glutamate release also affects neuronal networks by monitoring the spread of electrically evoked activity in slices loaded with a voltage-sensitive dye, RH141. Tumor-bearing acute brain slices from intracranially injected mice were stimulated peritumorally (Fig. 4A), and activity was recorded. Threshold stimulation evoked larger, longer lasting waves of depolarization as indicated by the greater mean amplitude and duration in slices containing SXC-expressing gliomas compared to sham control slices, whereas slices containing non-SXC-expressing gliomas displayed a slightly higher mean duration but not amplitude, versus control (Fig. 4B–E). The number of diodes activated in all glioma-implanted slices was significantly ($P<0.0001$) higher than sham-injected slices (Fig. 4F).

These findings suggest that functional SXC expression presents with peritumoral neuronal hyperexcitability. Therefore, we hypothesized that SXC expression may predict enhanced seizure susceptibility. To show this, we implanted 55 animals with either SXC-expressing (GBM22/GBM1066; red) or non-SXC-expressing (GBM14/GBM39; blue) gliomas and monitored brain activity by intracranial electroencephalogram (EEG). Continuous EEG monitoring for up to 23 days showed that 70–77% of mice implanted with the SXC-expressing gliomas developed seizures with epileptic discharges associated with tonic-clonic behavioral seizures lasting 30–120 seconds (Fig. 5, Movie S1). Although many of the glioma-implanted mice also exhibited interictal spike-wave epileptic discharges (Fig. 5, B, F), non-SXC-expressing glioma-implanted mice rarely had seizures, with only 3 out of 31 animals showing seizure events over an observation period of up to 23 days/animal, depending on survival (average survival 27.5 days for non-SXC-expressing glioma-implanted mice). Even for those rare events, SXC-expressing gliomas induced seizures earlier in the disease than non-SXC-expressing gliomas (Fig. 5E).

Genomic data stratify glioma patients

The above findings establish SXC expression as a predictor for excitotoxicity and seizure activity in mice implanted with human gliomas. To determine if this finding also holds true in glioma patients, we searched for evidence to correlate altered SLC7A11 expression with patient survival and seizure presentation. We extracted patient survival data from the NIH Repository for Molecular Brain Neoplasia Data (REMBRANDT) database(26), and divided the glioma patients included in the database into 2 groups, based on *SLC7A11* mRNA expression relative to non-neoplastic brain tissue (high *SLC7A11* expression, ≥150% mRNA expression; low *SLC7A11* expression, ≤ 66% mRNA expression). On average, patients with reduced *SLC7A11* expression lived 9 months longer than patients with tumors expressing elevated *SLC7A11* levels ($P=0.0238$, Log Rank Test) (Fig. 6A). This survival advantage may be due to decreased glutamate-mediated excitotoxicity, as a result of lower *SLC7A11* expression. Unfortunately, seizure status is not annotated for these patients.

SXC inhibition reduces peritumoral glutamate in patients

To extend these preclinical findings linking SXC to tumor-associated seizures and excitotoxicity, we explored whether glutamate release from gliomas can be attributed to SXC and hence modifiable using the FDA-approved SXC inhibitor sulfasalazine. In a pilot clinical study, we enrolled 9 patients and non-invasively measured changes in glutamate release by Magnetic Resonance Spectroscopy (MRS) as previously described (27). Because lower grade gliomas also express variable levels of SXC (fig. S11), this study included patients diagnosed with grade II–IV gliomas, including GBM, astrocytoma, and oligodendroglioma (3 patients each). For each patient, we measured the acute response of peritumoral glutamate (Glx) to acute oral dosing of sulfasalazine (SAS)(Fig. 6B, fig. S12). MRS data showed a range of Glx responses after SAS administration (Fig. 6C). Using chromogenic staining, we analyzed SLC7A11 expression in biopsy tissue from each patient and matched the SAS-induced response on MRS (Fig. 6, C–E). For each of the glioma subtypes, higher SLC7A11 expression predicted a larger change in Glx after each SAS dose. Indeed, SLC7A11 expression correlated significantly with the relative decrease in Glx for each GBM patient (Fig. 6E, $P=0.0134$; $R^2=0.9996$, linear regression). In patients with decreases in Glx after SAS, we observed a delayed increase in Glx 24 hours later (fig. S12B). This ‘rebound’ peak suggests that SXC activity and/or expression increases after pharmacological inhibition, consistent with glioma cells increasing their cystine uptake, and consequently, glutamate release, in an effort to resupply GSH after transient depletion.

In addition to MRS data, we were able to obtain EEG data for 6 of the 9 patients in the trial. EEGs were abnormal for all 6 patients, with findings ranging from focal or generalized slowing, breech rhythm, or epileptiform discharges to focal seizures (Fig. 6F, fig. S13). In 2/6 of these, the abnormal EEGs were obtained at times of clear tumor progression on imaging. Further patient information is included in Supplementary Table 1.

Discussion

Glioma glutamate release has been implicated in glioma growth(1, 10, 28), invasion(2, 29, 30), edema(31), and peritumoral epilepsy in animals(5), and some studies implicated the cystine/glutamate exchanger, SXC, as one of the glutamate release pathways in gliomas(31–33). SXC is universally upregulated in glioma cell lines, yet our analysis of human glioma tissue in TMAs unveiled a subpopulation of approximately 54% of glioma patients who have elevated tumor SLC7A11 expression, whereas the remaining 46% have lower expression, comparable to control brain levels. The subset of gliomas expressing elevated SXC corresponded well with the incidence of tumor-associated seizures reported in the glioma patient population(34). Moreover, we show that lack of SLC7A11 expression confers an improved clinical outcome for patients, who live on average 9 months longer.

Because the TMAs contained peritumoral brain from each patient, we were able to compare relative SLC7A11 expression of tumor against surrounding brain. Although this peritumoral brain tissue may contain a low density of invading tumor cells, which may falsely elevate the SLC7A11 expression in the peritumoral brain of patients with higher SLC7A11-expressing tumors, this comparison offers a reasonable internal control. Comparable expression differences were observed in patient glioma xenografts analyzed by Western

blot, and in those, SLC7A11 expression also correlated with glutamate release, determined through absorbance and radiotracer studies. Using 2 xenolines expressing very high and 2 xenolines expressing very low levels of SLC7A11, we had the opportunity to functionally study patient gliomas that natively express or lack SXC, and as a result, do or do not release glutamate. SXC expression was associated with extensive peritumoral neuronal death, mediated by NMDA-R induced excitotoxicity. Animals intracranially implanted with these gliomas frequently exhibited tumor-associated seizures, which were rare in animals implanted with gliomas lacking SXC. The absence of SXC was also associated with ~40% longer survival. These data strongly suggest that SXC-mediated glutamate release is causal of tumor-associated epilepsy.

The patient-derived xenoline glioblastoma model proved to be a clinically relevant model of the human disease, particularly because, unlike cell lines, they reproduced spontaneous seizures when implanted intracranially in mice. Both on video and EEG, these animals experienced events which resemble the more typical seizure activity seen in glioma patients(19), in contrast to previous studies of mice implanted with SXC-expressing glioma cell lines, which only show interictal spiking on EEG(5). The xenolines are known to prevent the genetic changes seen *in vitro*(21–23) and preserve the heterogeneous SLC7A11 expression found in patient TMAs. Although there appears to be a continuous distribution of SLC7A11 expression, it follows a bimodal pattern, where approximately half of the tumors express higher levels than surrounding brain tissue.

Our studies extend previous reports demonstrating glutamate release from glioma cell lines(31–33, 35), and toxic peritumoral glutamate concentrations in patients(1). Previously, the strongest evidence of SXC's role in this aspect of tumor biology was from a study using shRNA knockdown of *SLC7A11* in a glioma cell line. When these knockdown cells were implanted *in vivo*, peritumoral edema and neuronal death were reduced and overall survival was enhanced compared to control mice(32).

Both the heterogeneity of SLC7A11 expression in gliomas and the identification of two populations of gliomas with either reduced or enhanced SXC expression were unexpected, and the survival advantage for glioma patients based on genomic data in the REMBRANDT brain tumor database is compelling. In patients, reduced *SLC7A11* expression correlated with an average increase in survival of 9 months. Unfortunately, current tumor databases do not reliably record seizure incidence, and patient medication status is not a reliable indicator of seizure activity because many patients are prophylactically maintained on anti-epileptic drugs regardless of seizure status. Recent clinical studies have found correlations between increased SLC7A11 expression and seizure incidence(6) that agree with our findings, as well as faster tumor growth and worse prognosis for patients with increased tumor SLC7A11 expression(36). Of note, some contradictory findings suggest that new-onset seizures favor a better survival for patients, whereas a recurrence or worsening of seizures predicts tumor progression and therefore worse survival(37–39). Because most patients will seek medical evaluation for a new onset seizure, these patients may present earlier and subsequently be treated at an earlier time point. A loss of survival benefit with recurrence or worsening of tumor-associated seizures suggests that tumor growth may parallel seizure occurrence.

Our prospective clinical pilot study had no intent to treat but instead sought to show that glutamate release measured by MRS occurred via the SXC transporter and can therefore be modified by SAS. In the 9 patients tested, a spectrum of glutamate responses were seen after SAS administration, and the MRS glutamate response correlated with the extent of glioma SLC7A11 expression in each subtype of patient tumor. Gliomas of all grades variably express SXC (40). When present, it is likely to contribute to excitotoxicity and potential tumor-associated seizures, regardless of tumor grade. This agrees with studies showing increased peritumoral glutamate in patients harboring anaplastic astrocytoma(1) and oligodendroglioma(41). Because our functional studies focused only on high-grade gliomas, further exploration of SXC expression and function among low-grade gliomas is warranted.

Although underpowered to make broader claims, these data suggest that glutamate release from gliomas occurs principally via SXC, and that SAS penetrates the blood brain barrier and acutely reduces glutamate. Together with our preclinical data, this suggests that SXC activity accounts in large measure for tumor-associated seizures and peritumoral excitotoxicity. Future studies will need to examine whether SXC-mediated glutamate release measured by MRS may serve as a sensitive, non-invasive clinical marker to identify patients with excitotoxic tumors who will experience more rapid disease progression and seizure complications. This screening would also help identify patients who may benefit from adjuvant therapy targeting SXC inhibition.

Of note, SAS is an imperfect drug, because its biological half-life is only 80 min(19) and the majority of the drug is lost to cleavage by gut bacteria. However, it is currently the only approved drug targeting SXC. More specific SXC inhibitors with improved specificity and bioavailability are under development(42) and may soon enter clinical trials.

Together with past work, our findings provide a confluence of evidence to argue in favor of a growth-promoting and excitotoxicity-inducing role of SXC-mediated glutamate release from malignant gliomas. We identified a non-invasive way to detect SXC activity and resulting glutamate release in glioma patients. Similar glutamate spectroscopy may be instructive for other seizure disorders; these may potentially benefit from SAS and/or other drugs with similar mechanisms of action in the brain. Indeed, gliomas belong to the group of acquired/symptomatic epilepsies, which also include those resulting from trauma, infections, and brain abnormalities such as mesial-temporal lobe sclerosis. In each of these disorders, glial abnormalities have been demonstrated(43–48). It is possible, even likely, that elevated SXC expression in glial cells may contribute more generally to acquired epilepsy, with glioma being just an example in which this mechanism is being identified.

Materials and Methods

Study Design

The goal of this study was to determine the role of SXC-mediated glioma glutamate release in excitotoxicity/seizures. Experiments were performed on glioma tissue and tissue grown *in vivo* (approved by UAB Institutional Animal Care and Use Committee (IACUC)/UAB Institutional Review Board (IRB)). Sample sizes were determined based on previous publications(5, 33). For *in vivo* experiments, animals that did not establish a tumor were

excluded (per pre-established exclusion criteria). Naïve mice were randomly chosen for intracranial injections (same species/strain/age/sex and housing/maintenance conditions); endpoint was being moribund or death. *In vitro* experiments included ≥3 biological replicates and 2–4 technical replicates. Investigators were blinded during TMA SLC7A11 scoring, and also blinded to xenoline identity during EEG analysis and specific *in vitro* experiments (indicated in figure legends). The pilot clinical trial (ClinicalTrials.gov, #NCT01577966) was a randomized prospective trial, designed to test MRS detection of SXC activity through glutamate release. Nine patients with a histological diagnosis of malignant glioma were randomly recruited at UAB, and written consent was obtained. Separate investigators performed MRS analysis and chromogenic staining quantification, blinded to patient identity; data were matched after analysis was complete.

SLC7A11 IHC on GBM Invasion TMA

Face cuts from formalin-fixed, paraffin-embedded blocks of tissue from GBM patients were identified by board-certified neuropathologists as containing tumor core, edge, or rim (core: hypercellular, angiogenic areas; edge: interface between tumor core and peritumoral brain; rim: peritumoral brain). 1 mm tissue punches from marked regions were serially sectioned at 8 μm thickness(49). Using standard IHC processing protocols, sections were stained for SLC7A11 (1:25 dilution; Abcam), followed by a peroxidase-conjugated secondary antibody, with diaminobenzidine/hydrogen peroxide as chromogen/substrate. Scoring was based on a 0–3 staining intensity scale (matched areas of adjacent brain for each tissue sample used as reference for relative change of tumor versus peritumoral brain). Only tissues successfully processed for staining were analyzed (41/45 samples). Tumor cores consistently showed higher cellular density than tumor rim or peritumoral brain. Because of patient-to-patient variability, we did not attempt to establish correlation of SLC7A11 expression and cellular density.

Western Blot

Western blotting was performed as previously described(50).

Glutamate Release

Gliospheres were dissociated, and 2.5×10^6 cells were incubated in 2 ml medium ± inhibitor ((S)-4-CPG, 0.5 mM). Medium was collected after 24 h and glutamate concentrations measured using a Glutamate Assay Kit (Sigma-Aldrich), according to the manufacturer's directions.

Glutamate Uptake

Glutamate uptake procedures were performed as previously described(51). Reverse-mode uptake was performed to measure SXC activity(52). Dissociated cells were plated at 100,000 cells/well in 24-well plates.

Calcium Imaging

Calcium imaging and calibration were performed as previously described(53).

Retrospective analysis of SLC7A11 gene expression in human gliomas

Correlations between *SLC7A11* expression and patient survival were determined through analysis of the Repository for Molecular Brain Neoplasia Data (REMBRANDT, http://caintegrator.nci.nih.gov/rembrandt). High *SLC7A11* expression was defined as ≥150% increase, low was defined as ≥66% decrease in expression compared to mean non-neoplastic brain.

Immunohistochemistry

Tumor-implanted animals were perfused with PBS followed by 4% paraformaldehyde (PFA). 100 μm coronal sections were blocked for 1 hour at RT in blocking buffer (10% serum, 0.5% TritonX-100) and incubated with primary antibodies [anti-neuronal nucleic (NeuN)(1:500; Millipore), anti-glial fibrillary acid protein (GFAP) (1:1000; DAKO), anti-SLC7A11 (1:100; Abcam), or anti-human nuclei (HuN) (1:1000; Millipore)] 4°C, overnight. Slices were washed with PBS for 20 min and incubated with secondary antibodies [Alexa Fluor (1:1500; Invitrogen) for 1 hour at RT. Washed slices were mounted on glass slides and coverslipped using AquaPolymount (Polysciences). Images were acquired with an Olympus Fluoview FV1000 laser-scanning microscope (Olympus). Peritumoral neuronal density was quantified as the number of NeuN+ peritumoral neurons, normalized to the total peritumoral area (240–350 mm). NeuN staining showed autofluorescence in areas of necrosis. For HuN cell quantification, 25 ROIs (3 animals/condition) were imaged, and the number of cells migrating away from the tumor mass (≤300 μM distance from tumor border) was quantified.

In Vitro EEG/video recording

EEG and video recording was performed as previously described(5). Events 12–15 Hz and ≥5x baseline amplitude were flagged for analysis. EEG abnormalities were matched with video to confirm seizures. Animals were recorded until moribund.

Electrophysiology

Isoflurane-anesthetized animals were decapitated and brains immersed in ice-cold ACSF [(in mM): 135 NMDG, 1.5 KCl, 1.5 KH_2PO_4, 23 choline bicarbonate, 25 D-glucose, 0.5 $CaCl_2$, 3.5 $MgSO_4$]. Coronal slices (300 μm) were recovered for 1 h in ACSF [(in mM): 125 NaCl, 3 KCl, 1.25 NaH_2PO_4, 25 $NaHCO_3$, 2 $CaCl_2$, 1.3 $MgSO_4$, 25 glucose] at 37°. For whole-cell recordings of spontaneous postsynaptic currents (sPSC), cells were held at −70 mV. The intracellular solution contained [(in mM): 134 K-gluconate, 1 KCl, 10 HEPES, 2 Mg-ATP, 0.2 Na-GTP, and 0.5 EGTA, pH 7.4, 285–290 mOsm]. Tight seals were made with patch electrodes (KG-33 glass, Garner Glass) with a 3–5 MΩ open-tip resistance. Data were acquired using an Axopatch 200B amplifier, pClamp 10 software, and a Digidata 1440A interface (Molecular Devices). Data were filtered at 5 kHz, digitized at 10–20 kHz, and analyzed using Clampfit 10.0 software (Molecular Devices).

Voltage-sensitive Optical Recordings

Voltage-sensitive dye experiments were conducted as previously described(5) using the voltage-sensitive fluorescent dye RH414.

Proton Magnetic Resonance Spectroscopy

Imaging was performed on a 3T head-only MRI scanner (Siemens Allegra) with a circularly-polarized transmit/receive head coil. Anatomical localizer images (gradient-recalled echo sequence; TR/TE=250/3.48 milliseconds; flip angle, 70°; 5-mm slice thickness; 1.5-mm gap; 512×512 matrix) were acquired in axial/coronal/sagittal planes for spectroscopic voxel placement. Voxels (2×2×2 cm) were placed peritumorally in normal-appearing brain tissue. After manual shimming, water-suppressed spectra were acquired using the point-resolved spectroscopy sequence (PRESS; TR/TE=2000/80 milliseconds to optimize Glx signal and minimize macromolecule contribution; spectral band-width of 1200 Hz, 1024 points, 256 averages [8 minutes/30 seconds]).

Statistical Analysis

Results are presented as means ± SEM, unless otherwise indicated. Significance was defined as $P<0.05$. GraphPad Prism 5.02 and Origin 8.5 were used for statistical analysis. MRS data were analyzed with SPSS 12.0. The Shapiro-Wilk test for normality was used, and non-normally distributed data were subjected to a two-tailed Mann Whitney test. Normally distributed data were subjected to either a one-way ANOVA with Tukey Post-test, or two-tailed Student's *t*-test. For survival analysis, Kaplan-Meier analysis was performed followed by log-rank test. In Figure 1B, unimodality of the distribution of the individual groups was confirmed by the dip test of unimodality(54) using R.3.1.2 program with dip-test package installed (The R Foundation for Statistical Computing). Original data and exact p values shown in table S2.

Additional Methods

Detailed methodology is described in Supplementary Materials and Methods.

Supplementary Material

Refer to Web version on PubMed Central for supplementary material.

Acknowledgments

We thank UAB Brain Tumor Tissue Core Facility for providing human xenograft tissue, UAB Eunice Kennedy Shriver Intellectual and Developmental Disabilities Research Center supported by P30-HD38985, and the UAB Neuroscience Molecular Detection Core (NIH NS047466).

Funding: Supported by NIH grants 5R01NS052634, 2RO1NS036692, 5RO1NS031234, 1F31NS074597, 1R01NS082851, 5TL1RR025775-04, 2T32NS048039, T32GM008361 and T32GM008362. M.E.B. is supported by a grant from the Ben & Catherine Ivy Foundation.

References and Notes

1. Marcus HJ, Carpenter KL, Price SJ, Hutchinson PJ. In vivo assessment of high-grade glioma biochemistry using microdialysis: a study of energy-related molecules, growth factors and cytokines. J Neurooncol. 2010; 97:11–23. [PubMed: 19714445]
2. Ishiuchi S, et al. Blockage of Ca(2+)-permeable AMPA receptors suppresses migration and induces apoptosis in human glioblastoma cells. Nat Med. 2002; 8:971–978. [PubMed: 12172541]
3. Lai TW, Zhang S, Wang YT. Excitotoxicity and stroke: identifying novel targets for neuroprotection. Progress in neurobiology. 2014; 115:157–188. [PubMed: 24361499]

4. Bonova P, Burda J, Danielisova V, Nemethova M, Gottlieb M. Delayed postconditioning reduces post-ischemic glutamate level and improves protein synthesis in brain. Neurochemistry international. 2013; 62:854–860. [PubMed: 23454191]
5. Buckingham SC, et al. Glutamate release by primary brain tumors induces epileptic activity. Nat Med. 2011; 17:1269–1274. [PubMed: 21909104]
6. Yuen TI, et al. Glutamate is associated with a higher risk of seizures in patients with gliomas. Neurology. 2012; 79:883–889. [PubMed: 22843268]
7. Matthew E, Sherwin AL, Welner SA, Odusote K, Stratford JG. Seizures following intracranial surgery: incidence in the first post-operative week. The Canadian journal of neurological sciences Le journal canadien des sciences neurologiques. 1980; 7:285–290. [PubMed: 7214242]
8. van Breemen MS, et al. Efficacy of anti-epileptic drugs in patients with gliomas and seizures. Journal of neurology. 2009; 256:1519–1526. [PubMed: 19434440]
9. Wallace EM, O'Reilly M, Twomey M. A review of the use of antiepileptic drugs in high-grade central nervous system tumors. The American journal of hospice & palliative care. 2012; 29:618–621. [PubMed: 22363032]
10. de Groot J, Sontheimer H. Glutamate and the biology of gliomas. Glia. 2011; 59:1181–1189. [PubMed: 21192095]
11. Ogunrinu TA, Sontheimer H. Hypoxia increases the dependence of glioma cells on glutathione. The Journal of biological chemistry. 2010; 285:37716–37724. [PubMed: 20858898]
12. Robert SM, Ogunrinu-Babarinde T, Holt KT, Sontheimer H. Role of glutamate transporters in redox homeostasis of the brain. Neurochemistry international. 2014
13. Singh S, Khan AR, Gupta AK. Role of glutathione in cancer pathophysiology and therapeutic interventions. Journal of experimental therapeutics & oncology. 2012; 9:303–316. [PubMed: 22545423]
14. Sato H, Tamba M, Ishii T, Bannai S. Cloning and expression of a plasma membrane cystine/glutamate exchange transporter composed of two distinct proteins. The Journal of biological chemistry. 1999; 274:11455–11458. [PubMed: 10206947]
15. Benveniste H, Drejer J, Schousboe A, Diemer NH. Elevation of the extracellular concentrations of glutamate and aspartate in rat hippocampus during transient cerebral ischemia monitored by intracerebral microdialysis. Journal of neurochemistry. 1984; 43:1369–1374. [PubMed: 6149259]
16. Collins RC, Dobkin BH, Choi DW. Selective vulnerability of the brain: new insights into the pathophysiology of stroke. Annals of internal medicine. 1989; 110:992–1000. [PubMed: 2543255]
17. Ben-Ari Y. Limbic seizure and brain damage produced by kainic acid: mechanisms and relevance to human temporal lobe epilepsy. [review] [200 refs]. Neurosci. 1985; 14:375–403.
18. Olney JW, Collins RC, Sloviter RS. Excitotoxic mechanisms of epileptic brain damage. Advances in neurology. 1986; 44:857–877. [PubMed: 3706027]
19. Berkenbach F, et al. The Alzheimer's amyloid precursor protein is produced by Type I astrocytes in primary cultures of rat neuroglia. J Neurosci Res. 1990; 25:431–440. [PubMed: 2109094]
20. Shukla K, et al. Inhibition of transporter-mediated cystine uptake by sulfasalazine analogs. Bioorganic & Medicinal Chemistry Letters. 2011; 21:6184–6187. [PubMed: 21889337]
21. Leuraud P, et al. Correlation between genetic alterations and growth of human malignant glioma xenografted in nude mice. British journal of cancer. 2003; 89:2327–2332. [PubMed: 14676814]
22. Pandita A, Aldape KD, Zadeh G, Guha A, James CD. Contrasting in vivo and in vitro fates of glioblastoma cell subpopulations with amplified EGFR. Genes, chromosomes & cancer. 2004; 39:29–36. [PubMed: 14603439]
23. Giannini C, et al. Patient tumor EGFR and PDGFRA gene amplifications retained in an invasive intracranial xenograft model of glioblastoma multiforme. Neuro-oncology. 2005; 7:164–176. [PubMed: 15831234]
24. Hoffman WH, Haberly LB. Bursting induces persistent all-or-none EPSPs by an NMDA-dependent process in piriform cortex. The Journal of neuroscience: the official journal of the Society for Neuroscience. 1989; 9:206–215. [PubMed: 2563277]
25. Hoffman WH, Haberly LB. Bursting-induced epileptiform EPSPs in slices of piriform cortex are generated by deep cells. The Journal of neuroscience: the official journal of the Society for Neuroscience. 1991; 11:2021–2031. [PubMed: 1676726]

26. N. C. Institute. REMBRANDT home page. 2005. http://rembrandt.nci.nih.gov
27. Reid MA, et al. Assessments of function and biochemistry of the anterior cingulate cortex in schizophrenia. Biological psychiatry. 2010; 68:625–633. [PubMed: 20570244]
28. Ishiuchi S, et al. Ca2+-permeable AMPA receptors regulate growth of human glioblastoma via Akt activation. The Journal of neuroscience: the official journal of the Society for Neuroscience. 2007; 27:7987–8001. [PubMed: 17652589]
29. Piao Y, Lu L, de Groot J. AMPA receptors promote perivascular glioma invasion via beta1 integrin-dependent adhesion to the extracellular matrix. Neuro-oncology. 2009; 11:260–273. [PubMed: 18957620]
30. Lyons SA, Chung WJ, Weaver AK, Ogunrinu T, Sontheimer H. Autocrine glutamate signaling promotes glioma cell invasion. Cancer research. 2007; 67:9463–9471. [PubMed: 17909056]
31. Chung WJ, et al. Inhibition of cystine uptake disrupts the growth of primary brain tumors. The Journal of neuroscience: the official journal of the Society for Neuroscience. 2005; 25:7101–7110. [PubMed: 16079392]
32. Savaskan NE, et al. Small interfering RNA-mediated xCT silencing in gliomas inhibits neurodegeneration and alleviates brain edema. Nat Med. 2008; 14:629–632. [PubMed: 18469825]
33. Ye ZC, Sontheimer H. Glioma cells release excitotoxic concentrations of glutamate. Cancer research. 1999; 59:4383–4391. [PubMed: 10485487]
34. Kerkhof M, Vecht CJ. Seizure characteristics and prognostic factors of gliomas. Epilepsia. 2013; 54(Suppl 9):12–17. [PubMed: 24328866]
35. Takano T, et al. Glutamate release promotes growth of malignant gliomas. Nat Med. 2001; 7:1010–1015. [PubMed: 11533703]
36. Takeuchi S, et al. Increased xCT expression correlates with tumor invasion and outcome in patients with glioblastomas. Neurosurgery. 2013; 72:33–41. discussion 41. [PubMed: 23096413]
37. Vecht CJ, Kerkhof M, Duran-Pena A. Seizure prognosis in brain tumors: new insights and evidence-based management. The oncologist. 2014; 19:751–759. [PubMed: 24899645]
38. Wick W, et al. Pharmacotherapy of epileptic seizures in glioma patients: who, when, why and how long? Onkologie. 2005; 28:391–396. [PubMed: 16160401]
39. Chaichana KL, Parker SL, Olivi A, Quinones-Hinojosa A. Long-term seizure outcomes in adult patients undergoing primary resection of malignant brain astrocytomas. Clinical article. Journal of neurosurgery. 2009; 111:282–292. [PubMed: 19344222]
40. Stockhammer F, von Deimling A, van Landeghem FK. Decreased expression of the active subunit of the cystine/glutamate antiporter xCT is associated with loss of heterozygosity of 1p in oligodendroglial tumours WHO grade II. Histopathology. 2009; 54:241–247. [PubMed: 19207949]
41. Rijpkema M, et al. Characterization of oligodendrogliomas using short echo time 1H MR spectroscopic imaging. NMR in biomedicine. 2003; 16:12–18. [PubMed: 12577293]
42. Newell JL, et al. Novel di-aryl-substituted isoxazoles act as noncompetitive inhibitors of the system x cystine/glutamate exchanger. Neurochemistry international. 2013
43. Martinian L, et al. Expression patterns of glial fibrillary acidic protein (GFAP)-delta in epilepsy-associated lesional pathologies. Neuropathology and applied neurobiology. 2009; 35:394–405. [PubMed: 19508443]
44. Ludwin SK. Reaction of oligodendrocytes and astrocytes to trauma and implantation. A combined autoradiographic and immunohistochemical study. Laboratory investigation; a journal of technical methods and pathology. 1985; 52:20–30.
45. Eid T, Tu N, Lee TS, Lai JC. Regulation of astrocyte glutamine synthetase in epilepsy. Neurochemistry international. 2013; 63:670–681. [PubMed: 23791709]
46. Sosunov AA, et al. The mTOR pathway is activated in glial cells in mesial temporal sclerosis. Epilepsia. 2012; 53(Suppl 1):78–86. [PubMed: 22612812]
47. Lu C, et al. Elevated plasma S100B concentration is associated with mesial temporal lobe epilepsy in Han Chinese: a case-control study. Neuroscience letters. 2010; 484:139–142. [PubMed: 20727940]

48. Brenner M. Role of GFAP in CNS injuries. Neuroscience letters. 2014; 565:7–13. [PubMed: 24508671]
49. Kislin KL, McDonough WS, Eschbacher JM, Armstrong BA, Berens ME. NHERF-1: modulator of glioblastoma cell migration and invasion. Neoplasia (New York, NY). 2009; 11:377–387.
50. Cuddapah VA, et al. Kinase activation of ClC-3 accelerates cytoplasmic condensation during mitotic cell rounding. American journal of physiology Cell physiology. 2012; 302:C527–538. [PubMed: 22049206]
51. Ye ZC, Rothstein JD, Sontheimer H. Compromised glutamate transport in human glioma cells: reduction-mislocalization of sodium-dependent glutamate transporters and enhanced activity of cystine-glutamate exchange. The Journal of neuroscience: the official journal of the Society for Neuroscience. 1999; 19:10767–10777. [PubMed: 10594060]
52. Dun Y, et al. Expression of the cystine-glutamate exchanger (xc−) in retinal ganglion cells and regulation by nitric oxide and oxidative stress. Cell Tissue Res. 2006; 324:189–202. [PubMed: 16609915]
53. Cuddapah VA, Turner KL, Seifert S, Sontheimer H. Bradykinin-induced chemotaxis of human gliomas requires the activation of KCa3.1 and ClC-3. The Journal of neuroscience: the official journal of the Society for Neuroscience. 2013; 33:1427–1440. [PubMed: 23345219]
54. Hartigan JA, Hartigan PM. The Dip Test of Unimodality. Annals of Statistics. 1985; 13:70–84.
55. Bannai S. Exchange of cystine and glutamate across plasma membrane of human fibroblasts. The Journal of biological chemistry. 1986; 261:2256–2263. [PubMed: 2868011]
56. Seib TM, Patel SA, Bridges RJ. Regulation of the system x(C)− cystine/glutamate exchanger by intracellular glutathione levels in rat astrocyte primary cultures. Glia. 2011; 59:1387–1401. [PubMed: 21590811]
57. Giannini C, et al. Patient tumor EGFR and PDGFRA gene amplifications retained in an invasive intracranial xenograft model of glioblastoma multiforme. Neuro-oncology. 2005; 7:164–176. [PubMed: 15831234]
58. Jensen AM, Chiu SY. Fluorescence measurement of changes in intracellular calcium induced by excitatory amino acids in cultured cortical astrocytes. J Neurosci. 1990; 10:1165–1175. [PubMed: 1970355]
59. Iijima T, Mishima T, Akagawa K, Iwao Y. Mitochondrial hyperpolarization after transient oxygen-glucose deprivation and subsequent apoptosis in cultured rat hippocampal neurons. Brain research. 2003; 993:140–145. [PubMed: 14642839]
60. Williams SR, Christensen SR, Stuart GJ, Hausser M. Membrane potential bistability is controlled by the hyperpolarization-activated current I(H) in rat cerebellar Purkinje neurons in vitro. The Journal of physiology. 2002; 539:469–483. [PubMed: 11882679]
61. Naressi A, et al. Java-based graphical user interface for the MRUI quantitation package. Magma (New York, NY). 2001; 12:141–152.
62. Vanhamme L, van den Boogaart A, Van Huffel S. Improved method for accurate and efficient quantification of MRS data with use of prior knowledge. Journal of magnetic resonance (San Diego, Calif: 1997). 1997; 129:35–43.

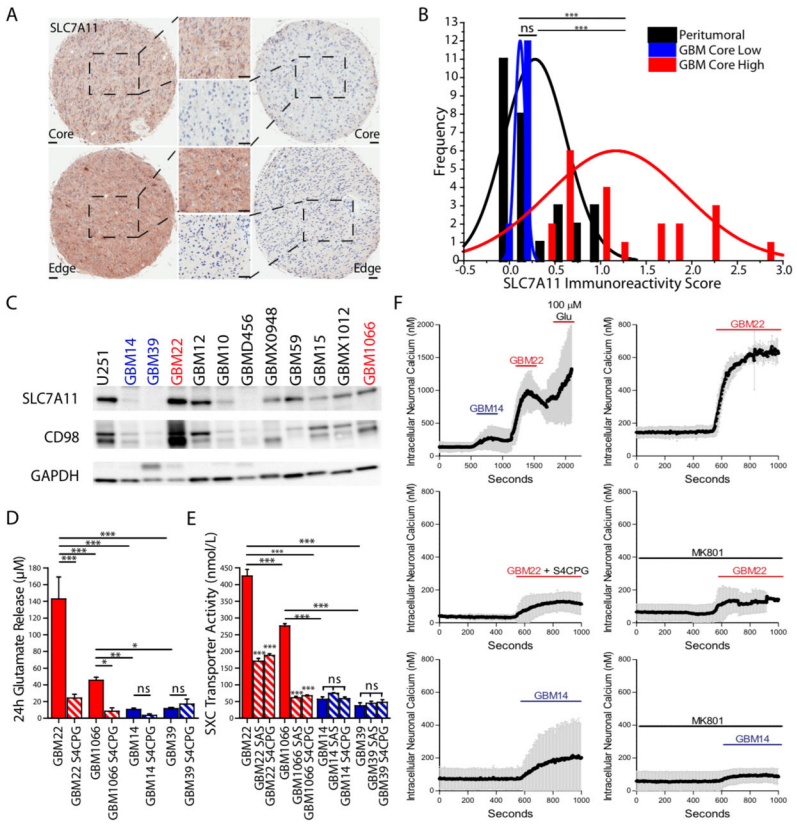

Fig. 1.

SXC is heterogeneously expressed in patient gliomas. (A) Representative examples of tissue microarrays (TMA) showing high (left) and low (right) SLC7A11 expression in tumor core (top) and edge (bottom) (*n*=41 patients). Center panels, higher magnification. Scale bars, 40 μm. (B) SLC7A11 immunoreactivity scores plotted as a function of frequency. Gaussian fits and testing for unimodality (Hartigans' dip test; Peritumoral expression, P=0.4757; GBM core expression, *P=0.01626), identify a significant departure from a unimodal population in the GBM core, segregating into low (blue; *n*=22 patients) and high (red; *n*=19 patients) SLC7A11 expression, relative to the average peritumoral brain expression (black; *n*=36 patients). Means ± SEM; ANOVA, Tukey's post-hoc test, ***P<0.0001, ns = not significant. (C) Western blot of SXC subunits (catalytic, SLC7A11; regulatory, CD98) in PDX-GBM samples ("GBM"), and a glioma cell line (U251); GAPDH, loading control, *n*=3 independent experiments. (D) Gliosphere medium glutamate concentrations, with or without (S)-4-CPG (*n*=3 independent experiments per condition). (E) SXC activity measured in reverse-transport mode, commonly used to measure transporter function(55, 56). Na^+-free glutamate uptake with or without SXC inhibitors (S)-4-CPG and sulfasalazine (SAS); *n*=3 independent experiments per condition. (D, E) Means ± SEM; ANOVA, Tukey's post-hoc test, *P<0.05, **P<0.01, ***P<0.0001, ns = not significant. (F) Fura-2 Ca^{2+}-imaging of cortical neurons in bath-applied, gliosphere-conditioned medium. Application of GBM14-conditioned medium was followed by GBM22 medium, then 100 μM glutamate. In separate experiments, g liosphere-conditioned medium was applied with or without a glutamate receptor inhibitor (MK-801), or a SXC inhibitor ((S)-4-CPG; *n*=3 independent experiments

per condition; 10–15 cells analyzed per experiment). (B–F) Red, higher SLC7A11 expression; blue, lower SLC7A11 expression.

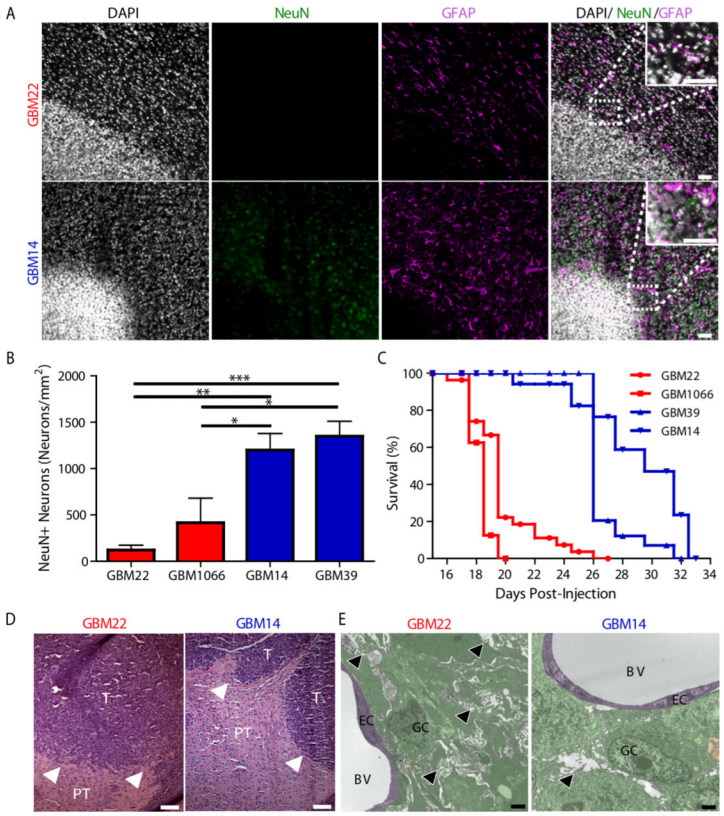

Fig. 2.

SXC-expressing gliomas induce peritumoral neuronal cell loss, edema, and decreased survival. (A) Immunofluorescence of nuclei (Dapi, white), peritumoral neurons (NeuN, green), and astrocytes (GFAP, magenta) in cortices implanted with SXC-expressing (GBM22) and non-SXC-expressing (GBM14) gliomas. Inset, 2.5x magnification; scale bars, 50 μm. (B) Peritumoral NeuN+ neuron quantification in the SXC-expressing (red) and non-SXC-expressing (blue) gliomas (*n*=3 animals per condition). Means ± SEM; ANOVA, Tukey's post-hoc test, *P<0.05, **P<0.01, ***P<0.0001. (C) Kaplan Meier plot of survival of tumor-bearing mice, days after injection for the SXC-expressing (GBM22, *n*=14 animals; GBM1066, *n*=10 animals) versus non-SXC-expressing (GBM14, *n*=15 animals; GBM39, *n*=16 animals) gliomas. (D) Representative H&E immunostaining of intracranially implanted SXC-expressing (GBM22; *n*=3 animals) and non-SXC-expressing (GBM14; *n*=3 animals) gliomas, highlighting less well defined borders of SXC-expressing gliomas, with finger-like projections invading into surrounding brain tissue (T = tumor, PT = peritumoral tissue; white arrowheads, tumor border). Scale bar, 100 μM. (E) Representative electron microscopy (EM) images showing cell morphology of SXC-expressing (GBM22, red; *n*=2 animals; 78 images analyzed) and non-SXC-expressing (GBM14, blue; *n*=2 animals; 46 images analyzed) intracranial gliomas. Tumoral and peritumoral edema (white areas, highlighted by black arrowheads) is apparent between the elaborately wound cellular processes of GBM22 cells. Less abundant, localized edema in GBM14 glioma-bearing cortex with more easily distinguished cell borders (right). GC = glioma cell(s)/processes

(green), EC = endothelial cell (purple), BV = blood vessel, black arrowhead = edema. Scale bar, 2 μM.

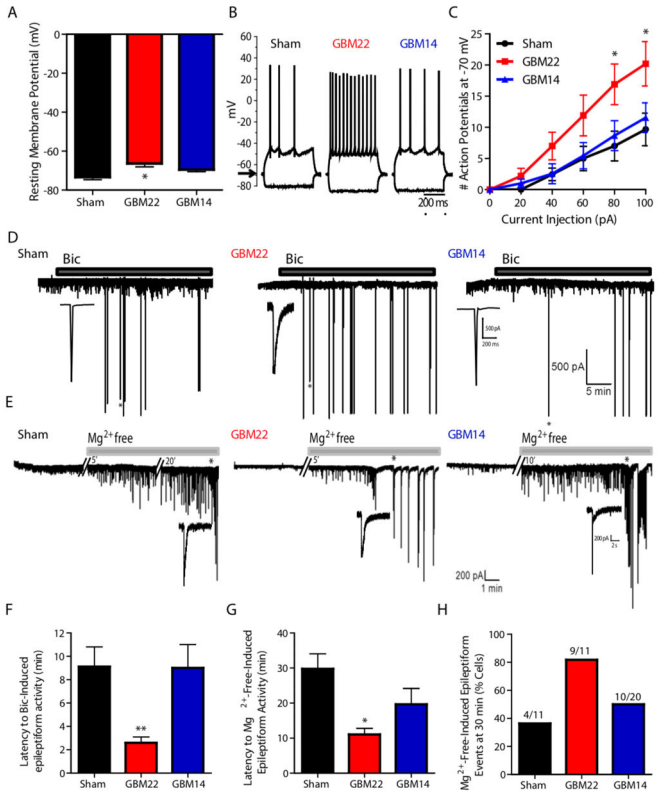

Fig. 3.

Neurons peritumoral to SXC-expressing tumors are hyperexcitable. (A) Whole-cell patch-clamp recordings of layer II/III pyramidal neurons showing the mean resting membrane potential (RMP) of neurons in sham-injected control mice (Sham, black; *n*=18 neurons) versus peritumoral neurons in SXC-expressing (GBM22, red; *n*=23 neurons) and non-SXC-expressing (GBM14, blue; *n*=16 neurons) glioma-implanted cortex. (B) Representative recordings of whole-cell current-clamp recordings in response to −100 and +100 pA current injection (held at −70 mV), in neurons from sham-injected mice (Sham, black; *n*=19 neurons), and neurons peritumoral to SXC-expressing (GBM22, red; *n*=16 neurons) and non-SXC-expressing (GBM14, blue; *n*=16 neurons) glioma-implanted cortex. (C) Number of action potentials fired in response to depolarizing current steps applied from 0 – 100 pA in 20 pA increments (neurons held at −70 mV), in sham-injected controls (Sham, black; *n*=18 neurons), and peritumoral to SXC-expressing (GBM22, red; *n*=16 neurons) and non-SXC-expressing (GBM14, blue; *n*=16 neurons) glioma-implanted cortex. (A–C) Means ± SEM; ANOVA, Tukey's post-hoc test compared to sham, *P<0.05. (D) Representative recordings of epileptiform activity induced by 10 μM bicuculline (Bic), in sham-injected controls (Sham, black; *n*=5 neurons), and neurons peritumoral to SXC-expressing (GBM22, red; *n*=4 neurons) and non-SXC-expressing (GBM14, blue; *n*=3 neurons) glioma-implanted cortex. *Individual epileptiform event on expanded time scale. (E) Sample recordings of epileptiform activity induced by magnesium-free ACSF in sham-injected controls (Sham, black; *n*=9 neurons), and neurons peritumoral to SXC-expressing (GBM22, red; *n*=7 neurons) and non-SXC-expressing (GBM14, blue; *n*=11 neurons) glioma-implanted cortex. *Indicates trace expanded in inset. (F) Latency to bicuculline-induced epileptiform activity

in sham-injected controls (Sham, black; *n*=5 neurons), and neurons peritumoral to SXC-expressing (GBM22, red; *n*=4 neurons) and non-SXC-expressing (GBM14, blue; *n*=4 neurons) glioma-implanted cortex. (G) Latency to magnesium-free-induced epileptiform activity in sham-injected controls (Sham, black; *n*=9 neurons), and neurons peritumoral to SXC-expressing (GBM22, red; *n*=7 neurons) and non-SXC-expressing (GBM14, blue; *n*=11 neurons) glioma-implanted cortex. (F, G) Means ± SEM; ANOVA, Tukey's post-hoc test compared to sham, *P<0.05, **P<0.01. (H) Percentage of neurons displaying epileptiform events at 30 min after magnesium-free ACSF was applied to sham-injected control slices (Sham, black; *n*=4/11 neurons) and neurons peritumoral to SXC-expressing (GBM22, red; *n*=9/11 neurons) and non-SXC-expressing (GBM14, blue; *n*=10/20 neurons) glioma-implanted cortex.

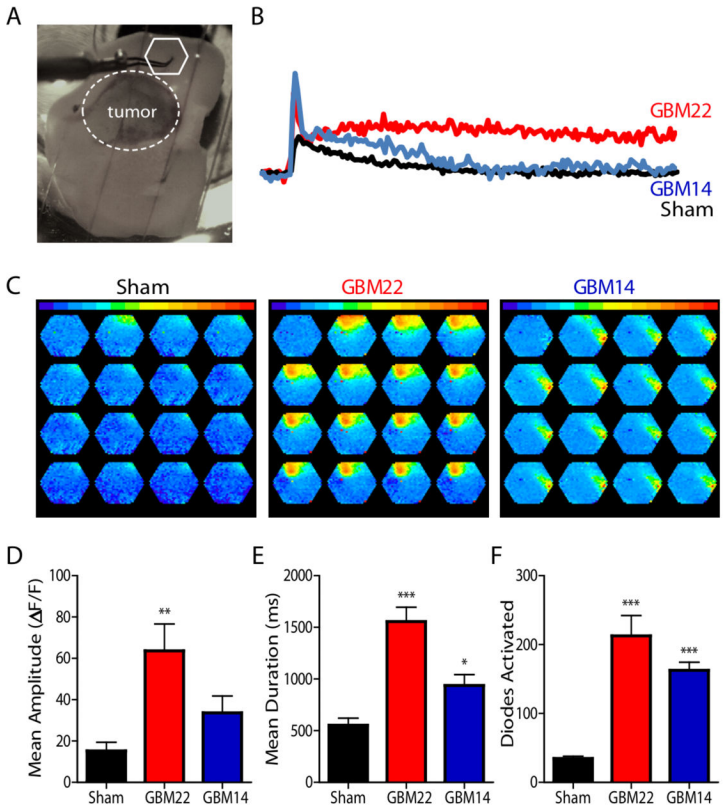

Fig. 4.

SXC-expressing gliomas create a hyperexcitable peritumoral network. Network excitability of glioma-bearing acute brain slices was detected by the voltage-sensitive fluorescent indicator RH-141. (A) Image illustrates placement of peritumoral recording electrode (white hexagon; white dotted circle defines tumor border). (B) Examples of individual diode responses and (C) spread of stimulus-induced activity in SXC-expressing (GBM22, red; *n*=3 animals) and non-SXC-expressing (GBM14, blue; *n*=3 animals) intracranially-implanted acute slices. Amplitude (D), duration (E), and number of diodes activated (F) during the response to threshold stimulation detected in GBM22 and GBM14 glioma-bearing acute slices, compared to sham-injected control animals (sham). (E–F) Means ± SEM; ANOVA, Tukey's post-hoc test, *P<0.05, **P<0.01, ****P*<0.0001. 5 ms intervals.

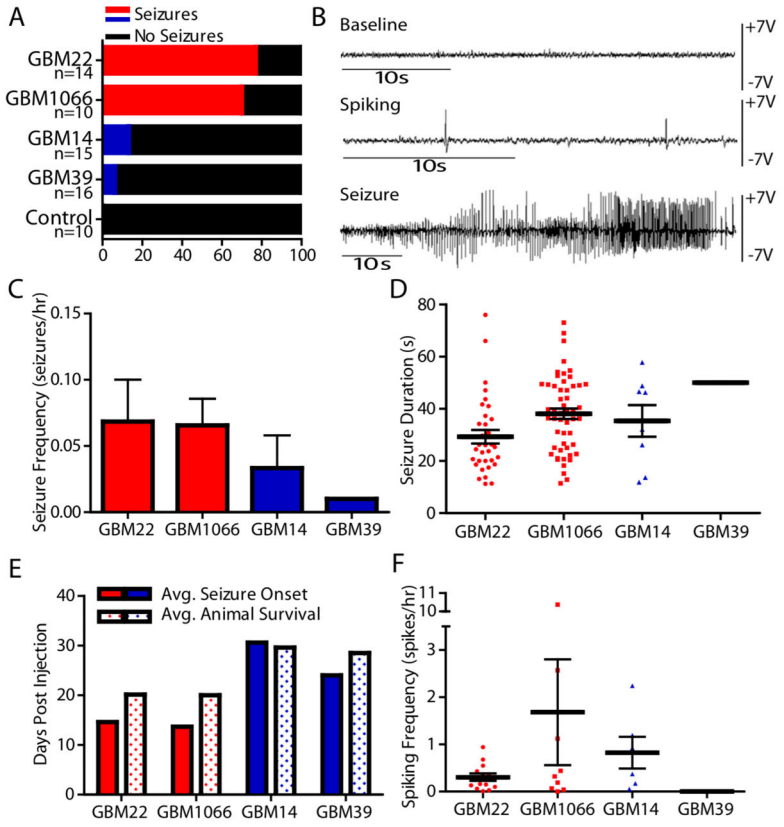

Fig. 5.

SXC-expressing gliomas cause seizures in vivo. (A) Percent of mice displaying EEG seizure activity (animals with ≥1 seizure(s) included in analysis; seizures confirmed by video monitoring) after intracranial implantation of SXC-expressing (Red; GBM22, *n*=14 animals; GBM1066, *n*=10 animals) versus non-SXC-expressing (Blue; GBM14, *n*=15 animals; GBM39, *n*=16 animals) gliomas. (B) Examples of *in vivo* EEG recordings of baseline (Baseline), interictal spike-wave epileptic discharges (Spiking), and seizure activity (Seizure) corresponding to tonic-clonic seizure activity. Seizure frequency (C) and duration (D) were calculated on the basis of recorded hours after the onset of the first seizure ((40 – 150 hours, depending on time of first seizure and recorded until animal death). Seizure duration includes all seizure activity recorded for each animal (2 status epilepticus events in GBM22-implanted animals were not included because the duration could not be accurately determined). (E) Comparison of the average day of initial seizure activity (Avg. Seizure Onset) versus average animal survival (Avg. Animal Survival) after intracranial injection (days post-injection). (F) Interictal spike-wave activity (Spiking) frequency calculated based on the number of recorded hours after the onset of initial interictal spike-wave activity. (C–F) Only animals with EEG/video-confirmed seizures were included in the analysis: GBM22, 13/14 animals; GBM1066, 7/10 animals; GBM14, 2/15 animals; GBM39, 1/16 animals). Meaningful statistics could not be performed because only a small number of non-SXC-expressing glioma-implanted animals had seizures or interictal spike-wave activity (GBM14, *n*=2 animals, 8 seizure events, 6 interictal spike-wave activity; GBM39, *n*=1

animals, 1 seizure event, 0 interictal spike-way activity) compared to SXC-expressing tumor-implanted animals.

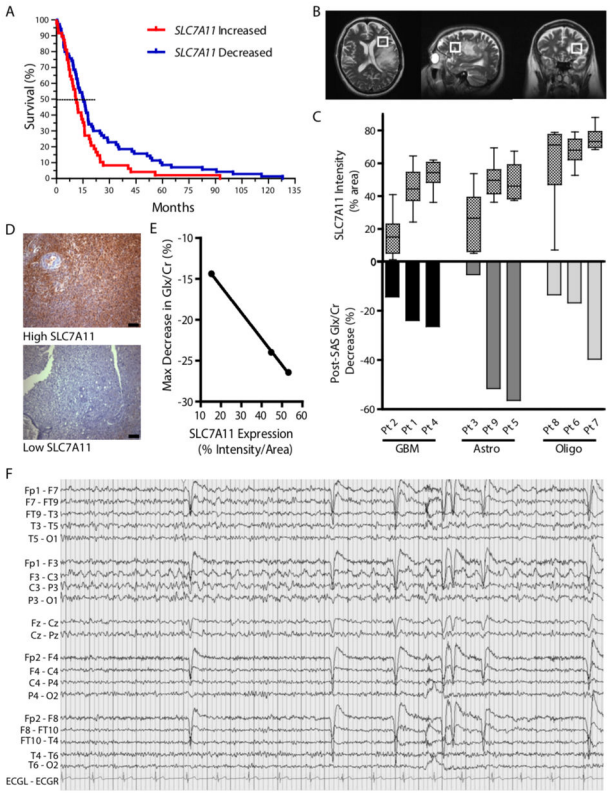

Fig. 6.

Glioma SXC expression predicts patient survival and peritumoral glutamate response. (A) Kaplan Meier survival plot of patients in the Repository for Molecular Brain Neoplasia Data (REMBRANDT) database comparing gliomas with high *SLC7A11* (≥150%) versus low expression (≤ 66%) of the SXC gene *SLC7A11*, compared to non-neoplastic brain (*n*=120 glioma (all grades) patients; Kaplan Meier analyzed using the log-rank test, P=0.0238). (B–E) Detection of peritumoral glutamate (Glx) measured by Magnetic Resonance Spectroscopy (MRS) in glioma patients before and after an acute sulfasalazine (SAS) dose (1 g). (B) Representative images showing voxel placement. (C) Peritumoral glutamate, detected as a peak composed of glutamate + glutamine (Glx), which is predominately glutamate(27), and quantified with respect to creatine (Cr). Intracranial Glx/Cr changes after SAS administration (Post-SAS) are graphed (bottom) and compared to SLC7A11 expression in patient glioma tissue (top) quantified by staining intensity (*n*=3 tissue samples per patient, total *n*=27; glioma types include glioblastoma (GBM), Astrocytoma (Astro), and Oligodendroglioma/Oligoastrocytoma (Oligo); Means ± SEM; ANOVA, P<0.0001). (D) Examples of high and low SLC7A11 staining of patient glioma tissue. Scale bars, 100 μM. (E) Linear correlation between maximum Glx/Cr decrease and GBM tissue SLC7A11 expression (Linear regression; *P=0.0134; R^2=0.9996). (F) Tracing of ictal discharge from Pt. 8, showing left centroparietal focal seizure best appreciated in leads F3/C3 and C3/P3. High-frequency filter (HFF) = 30 Hz; timebase = 15 mm/sec.

Table 1

Electrophysiology Results

	Sham	(n)	GBM22	(n)	GBM14	(n)
Resting membrane potential, mV	−73.0 ± 1.30	(18;4)	−66.4 ± 1.70	(23;5)**	−69.5 ± 1.10	(16;8)
Firing threshold, mV	−49.0 ± 1.20	(19;5)	−49.0 ± 0.88	(16;6)	−48.0 ± 1.04	(16;7)
Input resistance, MΩ	108 ± 12.0	(16;4)	152 ± 14.0	(22;4)	153 ± 13.0	(14;7)
Action potential amplitude, mV	79.0 ± 3.00	(13;5)	72.0 ± 3.00	(14;7)	73.0 ± 3.00	(13;10)
Action potential half width, ms	1.3 ± 0.06	(12;4)	1.20 ± 0.06	(16;9)	1.20 ± 0.20	(13;10)
AHP amplitude, mV	8 ± 1.60	(14;4)	7.90 ± 1.20	(16;8)	10.0 ± 1.50	(13;10)
Sag, mV	1.9 ± 0.30	(13;5)	4.00 ± 0.90	(15;8)	1.80 ± 0.50	(13;11)

Data are presented as mean ± s.e.m.; analyzed by ANOVA, Tukey's post hoc test vs sham;

** $P < 0.010$ (n) = (number of individual neurons; number of individual animals)